Crossover from *XY* critical to tricritical behavior of heat capacity at the smectic-*A*–chiral-smectic-*C* liquid-crystal transition

Kenji Ema and Haruhiko Yao
Department of Physics, Faculty of Science, Tokyo Institute of Technology 2-12-1 Oh-okayama, Meguro, Tokyo 152, Japan
(Received 18 December 1997)

High-resolution ac calorimetric measurements have been carried out for four chiral liquid-crystal systems: 4-(1-methylheptyloxycarbonyl) phenyl 4′-octyloxybiphenyl-4-carboxylate, its octylbiphenyl analog, its octyloxycarbonylbiphenyl analog, and 2-fluoro-4-{[(1-trifluoromethyl) undecyloxy] carbonyl} phenyl 4′-(dodecyloxy) biphenyl-4-carboxylate. The heat capacity anomaly around the smectic-*A* to the chiral-smectic-*C* transition has been analyzed in detail. It is revealed that the heat anomaly shows a crossover from three-dimensional *XY* critical to tricritical behavior. All the data are described well with a crossover function which has been obtained by a Rudnick-Nelson type calculation. [S1063-651X(98)14105-3]

PACS number(s): 61.30.−v, 64.70.Md, 64.60.Fr, 65.20.+w

I. INTRODUCTION

The study of critical behavior at the liquid-crystalline smectic-*A* (Sm-*A*) to smectic-*C* (Sm-*C*) or chiral smectic-*C* (Sm-*C**) transition has been an active area of research. The main motivation is that this transition is theoretically expected to belong to the three-dimensional (3D) *XY* universality class [1]. Early experimental studies revealed that these transitions exhibit mean-field behavior and are well described by Landau theory which includes the sixth-order term in the tilt order parameter [2–5]. Safinya *et al.* [6] showed that a simple argument with the Ginzburg criterion [7] indicates that the true critical region should be unobservably small for most Sm-*A*–Sm-*C* transitions. On the other hand, we recently found that the heat capacities of 4-(1-methylheptyloxycarbonyl)phenyl 4′-octyloxybiphenyl-4-carboxylate (MHPOBC) [8] and some related materials [9,10] show a clear deviation from the Landau behavior at Sm-*A*–Sm-C_α^* transition. Here, the Sm-C_α^* phase is an antiferroelectric version of the Sm-*C** phase. Further, it was found that the observed heat-capacity anomalies close to the transition are described by the 3D *XY* renormalization expression. A non-Landau behavior was also reported by Reed *et al.* for the heat capacity near the Sm-*A*–Sm-*C* transition of 5-*n*-decyl-2-[4-*n*-(perfluoropentyl-metheleneoxy) phenyl] pyrimidine (H10F5MOPP) [11].

A very interesting feature of many Sm-*A*–Sm-*C* transitions is the closeness to a tricritical point, which has been seen not only for the earlier Landau-like transitions (see Ref. [4], and references therein) but also for the recently found non-Landau transitions [11,12]. In particular, it is quite probable that the latter transitions can exhibit crossover from 3D *XY* critical to tricritical behavior. While theoretical approaches describing crossover phenomena from tricritical to ordinary critical behavior have been quite successful [13,14], experimental verification of theoretical predictions has been quite limited. The metamagnets $FeCl_2$ [15] and $Dy_3Al_5O_{12}$ [16] are such examples for Ising systems. The ^{3}He-^{4}He mixture is the only *XY* system for which detailed analyses of the crossover behavior have been made [17,18]. The nematic (*N*) to smectic-*A* (Sm-*A*) liquid-crystal transition is another example of a three-dimensional *XY* system which also exhibits tricritical behavior. However, measurements of heat capacity and correlation length have revealed that the data are well described by a single effective exponent value over a wide temperature range, suggesting that the crossover is very broad [19–23]. In addition, the crossovers both in ^{3}He-^{4}He and some of the *N*–Sm-*A* liquid crystals mentioned above are complicated by Fisher renormalization [24] which is inherent to some mixtures [25]. In this respect, the MHPOBC-group liquid crystals have an advantage that they are pure systems and are free from Fisher renormalization.

In this paper we report the results of the crossover-scaling analyses of our recent heat-capacity data on four liquid-crystal systems that exhibit Sm-*A*–Sm-*C** phase transitions. It is found that the heat-capacity anomaly at the Sm-*A*–Sm-*C** transition shows a universal crossover from 3D *XY* critical to Gaussian tricritical behavior as a function of reduced temperature.

The chiral liquid-crystal systems studied here are as follows. (1) 4-(1-methylheptyloxycarbonyl) phenyl 4′-octyloxybiphenyl-4-carboxylate, which exhibits the following phase sequence [26]:

$$\text{Sm-}C_A^* \overset{391.6\text{ K}}{\leftrightarrow} \text{Sm-}C_\gamma^* \overset{392.4\text{ K}}{\leftrightarrow} \text{Sm-}C^*$$

$$\overset{394.1\text{ K}}{\leftrightarrow} \text{Sm-}C_\alpha^* \overset{395.2\text{ K}}{\leftrightarrow} \text{Sm-}A \overset{421\text{ K}}{\leftrightarrow} I.$$

Here Sm-C_A^* and Sm-C_α^* are antiferroelectric phases, Sm-*C** is a ferroelectric phase, and Sm-C_γ^* is a ferrielectric phase, respectively. (2) 4-(1-methylheptyloxycarbonyl) phenyl 4′-octylbiphenyl-4-carboxylate (MHPBC), which exhibits the following phase sequence [27]:

$$\text{Sm-}C_A^* \overset{338.2\text{ K}}{\leftrightarrow} \text{Sm-}C_\gamma^* \overset{339.6\text{ K}}{\leftrightarrow} \text{AF} \overset{345.3\text{ K}}{\leftrightarrow} \text{Sm-}C_\alpha^*$$

$$\overset{349.5\text{ K}}{\leftrightarrow} \text{Sm-}A \overset{382.2\text{ K}}{\leftrightarrow} I.$$

TABLE I. Chemical structures of materials used.

MHPOBC	$C_8H_{17}O$-Ph-Ph-COO-Ph-$COOC^*H(CH_3)C_6H_{13}$
MHPBC	C_8H_{17}-Ph-Ph-COO-Ph-$COOC^*H(CH_3)C_6H_{13}$
MHPOCBC	$C_8H_{17}COO$-Ph-Ph-COO-Ph-$COOC^*H(CH_3)C_6H_{13}$
12BIMF10	$C_{12}H_{25}O$-Ph-Ph-COO-Ph(F)-$COOC^*H(CF_3)C_{10}H_{21}$

Here, AF is an antiferrielectric phase. (3) 4-(1-methylheptyloxycarbonyl) phenyl 4′ -octyloxycarbonyl-biphenyl-4-carboxylate (MHPOCBC), which exhibits the following phase sequence [28]:

$$\text{Sm-}C_A^* \overset{372.7\text{ K}}{\leftrightarrow} \text{Sm-}C_\alpha^* \overset{378.7\text{ K}}{\leftrightarrow} \text{Sm-}A \overset{420\text{ K}}{\leftrightarrow} I.$$

(4) 2-fluoro-4-{[(1-trifluoromethyl) undecyloxy] carbonyl} phenyl 4′-(dodecyloxy) biphenyl-4-carboxylate (12BIMF10), which exhibits the following phase sequence [29]:

$$\text{Sm-}C_A^* \overset{325.6\text{ K}}{\leftrightarrow} \text{Sm-}X^* \overset{326.6\text{ K}}{\leftrightarrow} \text{Sm-}C_\alpha^* \overset{328.6\text{ K}}{\leftrightarrow} \text{Sm-}A \overset{342.8\text{ K}}{\leftrightarrow} I.$$

Here, Sm-X^* is a ferrielectric phase. Chemical structures of these four materials are shown in Table I. Preliminary analysis of the data for MHPOBC and 12BIMF10 has appeared previously [30].

II. METHOD AND RESULTS

The heat capacity was measured using an ac calorimeter as described elsewhere [8,31]. Hermetically sealed gold cells which contained 30–50 mg of liquid-crystal sample were used. Temperature scan rate was about 0.03 K/h in the transition region. Very slow drift rates in the Sm-A–Sm-C_α^* transition temperature (-5 mK/day in MHPOBC, -2.4 mK/day in MHPOCBC, and within ± 1 mK/day in MHPBC and 12BIMF10) indicate the stability and high quality of the sample. The excess heat capacity ΔC_p is obtained as

$$\Delta C_p = C_p - C_p(\text{background}), \tag{1}$$

where C_p(background) is the background heat capacity determined as a quadratic function of the temperature which joins the observed heat-capacity data smoothly at temperatures away from the transition on both sides. Thus obtained ΔC_p has been plotted in the vicinity of the Sm-A–Sm-C_α^* transition in Figs. 1–4. Preliminary reports of the data on MHPOBC, MHPOCBC, and 12BIMF10 have been published previously [8–10,32]. Small anomalies are observed at 394.8 K and 392.8 K in MHPOBC, and at 326.9 K in 12BIMF10, which are due to the restructuring transitions between the chiral smectic-C phases, i.e., Sm-C_α^*–Sm-C^*, Sm-C^*–Sm-C_γ^*, and Sm-C_α^*–Sm-X^* phase transitions, respectively (the anomaly at 392.8 K in MHPOBC lies outside the temperature range of Fig. 1). To avoid the possibility that these anomalies might affect the analyses, the data in

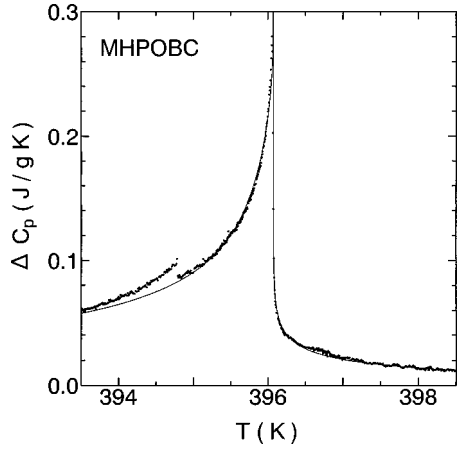

FIG. 1. Temperature dependence of the anomalous heat capacity ΔC_p of MHPOBC. The solid line is a fit to the data with the crossover expression given in Eqs. (3) and (4).

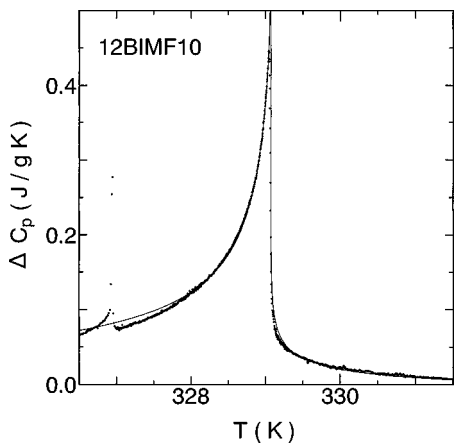

FIG. 2. Temperature dependence of the anomalous heat capacity ΔC_p of 12BIMF10. The solid line is a fit to the data with the crossover expression given in Eqs. (3) and (4).

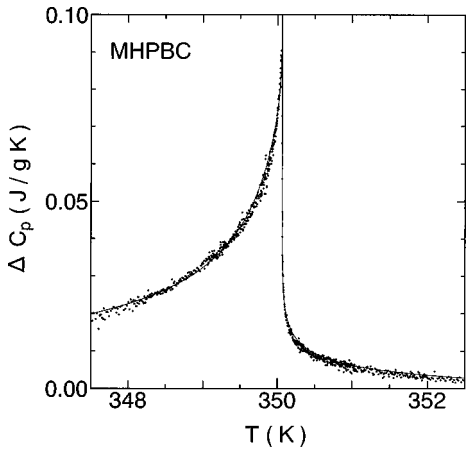

FIG. 3. Temperature dependence of the anomalous heat capacity ΔC_p of MHPBC. The solid line is a fit to the data with the crossover expression given in Eqs. (3) and (4).

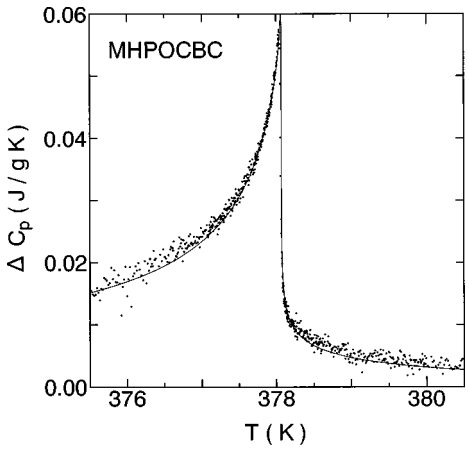

FIG. 4. Temperature dependence of the anomalous heat capacity ΔC_p of MHPOCBC. The solid line is a fit to the data with the crossover expression given in Eqs. (3) and (4).

ranges $391.8\ \mathrm{K}<T<392.8\ \mathrm{K}$ and $393.8\ \mathrm{K}<T<394.8\ \mathrm{K}$ in MHPOBC, and the data in a range $325.9\ \mathrm{K}<T<327.1\ \mathrm{K}$ in 12MIMF10 have been excluded in the fitting.

III. ANALYSIS

First, the ΔC_p data have been analyzed with the following renormalization-group expression including the corrections-to-scaling terms [33,34]:

$$\Delta C_p=\frac{A^{\pm}}{\alpha}|t|^{-\alpha}(1+D_1^{\pm}|t|^{\theta}+D_2^{\pm}|t|)+B_c\,, \qquad (2)$$

where $t\equiv(T-T_c)/T_c$ and the superscripts $\pm$ denote above and below T_c. The exponent α, and also T_c were adjusted freely in this least-squares fitting procedure. The correction-to-scaling exponent θ is actually dependent on the universality class, but has a theoretically predicted value quite close to 0.5 [33,35]. Therefore its value is fixed at 0.5 in this fitting. There is usually a narrow region very close to T_c where data are artificially rounded due to impurities or instrumental effects. The extent of this region was determined in the way described elsewhere [36], and data inside this region were excluded in the fitting. The rounding region thus determined is $-4\times10^{-5}<t<+1\times10^{-5}$ for MHPOBC and MHPBC, $-7\times10^{-5}<t<+1\times10^{-5}$ for MHPOCBC, and $-10\times10^{-5}<t<+1\times10^{-5}$ for 12BIMF10.

Table II shows the values of the critical exponent α and other adjustable parameters thus obtained. For these fits, the second-order correction coefficients $D_2^{\pm}$ were fixed at zero. Fits were made to the data over several ranges, and the maximum value of $|t|$ used in the fit, denoted as $|t|_{\max}$, is shown in the table. It is seen that the α value depends significantly on the fitting range, indicating that ΔC_p shows a crossover behavior. In particular, α seems to approach the 3D *XY* value $\alpha_{XY}=-0.0066$ [33] in the small $|t|_{\max}$ limit, while it moves in the direction of the tricritical value $\alpha_t=0.5$ for larger $|t|_{\max}$. Another trend is a violation of the scaling pre-

TABLE II. Least-squares values of the adjustable parameters for fitting ΔC_p with Eq. (2). Here, $\nu=N-p$, with N being the number of data points and p the number of free parameters. The units for A^+ and B_c are $\mathrm{J\,K^{-1}\,g^{-1}}$.

System	$\lvert t\rvert_{\max}$	T_c (K)	α	10^3A^+	A^-/A^+	D_1^+	D_1^-	B_c	ν	χ^2_ν
MHPOBC	0.0003	396.069	−0.002	26.046	0.982	−0.123	0.253	12.8315	34	1.07
	0.0005	396.070	0.062	11.552	1.649	2.382	−4.185	−0.2760	64	1.07
	0.001	396.070	0.087	8.913	1.918	3.292	−4.177	−0.1743	138	0.99
	0.003	396.072	0.158	3.1894	3.389	−2.138	−6.415	−0.0244	422	1.52
	0.01	396.072	0.210	1.7171	4.651	−11.89	−6.885	0.0099	825	2.04
12BIMF10	0.0005	329.071	0.028	31.387	1.296	1.680	−2.879	−1.3847	94	1.55
	0.001	329.072	0.102	11.683	2.424	3.268	−6.693	−0.2136	199	1.29
	0.003	329.073	0.177	4.2277	4.415	−4.049	−8.591	−0.0299	532	1.47
	0.01	329.074	0.229	2.4504	5.836	−11.56	−8.654	0.0079	1062	2.84
MHPBC	0.001	350.064	0.018	7.904	1.128	0.816	−0.630	−0.4992	222	1.37
	0.003	350.065	0.064	3.9937	1.574	1.369	−2.276	−0.0911	513	0.97
	0.01	350.065	0.094	2.7048	1.943	0.841	−3.085	−0.0461	861	0.86
MHPOCBC	0.001	378.072	0.004	3.5227	1.053	0.131	−0.568	−0.9014	226	1.00
	0.003	378.074	0.084	1.0588	2.736	−2.516	−6.537	−0.0134	460	1.30
	0.01	378.073	0.120	0.8903	3.121	−1.804	−5.466	−0.0088	800	2.07

TABLE III. Least-squares values of the adjustable parameters for fitting ΔC_p with Eq. (2). In these fits, the exponent values were fixed to 3D XY values, $\alpha=-0.0066$, and $\theta=0.524$. Quantities in brackets were held fixed at the given values. The units for A^+ and B_c are J K^{-1} g^{-1}.

System	$\lvert t\rvert_{\max}$	T_c (K)	10^3A^+	A^-/A^+	D_1^+	D_1^-	D_2^+	D_2^-	B_c	χ_ν^2
MHPOBC	0.001	396.062	35.606	0.961	−0.450	0.278	[0]	[0]	5.1263	1.84
	0.003	[396.062]	32.100	0.961	−0.299	0.264	[0]	[0]	4.6387	9.07
	0.01	[396.062]	29.340	0.966	−0.167	0.166	[0]	[0]	4.2598	30.9
	0.003	[396.062]	37.778	0.961	−0.686	0.341	4.80	−2.59	5.4265	1.33
	0.01	[396.062]	28.985	0.953	−0.387	0.617	1.73	−3.65	4.1902	3.54
12BIMF10	0.001	329.062	62.671	0.957	−0.458	0.410	[0]	[0]	9.0065	2.71
	0.003	[329.062]	60.458	0.961	−0.320	0.308	[0]	[0]	8.7128	17.08
	0.01	[329.062]	58.128	0.967	−0.203	0.198	[0]	[0]	8.4076	58.9
	0.003	[329.062]	63.443	0.955	−0.656	0.622	4.41	−4.58	9.1043	1.25
	0.01	[329.062]	59.282	0.957	−0.444	0.542	1.94	−3.12	8.5341	5.63
MHPBC	0.001	350.064	10.892	0.957	−0.384	0.296	[0]	[0]	1.5716	1.40
	0.003	[350.064]	10.111	0.957	−0.262	0.282	[0]	[0]	1.4631	1.43
	0.01	[350.064]	9.923	0.961	−0.179	0.212	[0]	[0]	1.4394	2.82
	0.003	[350.064]	11.474	0.958	−0.569	0.314	3.80	−1.74	1.6526	0.94
	0.01	[350.064]	10.165	0.955	−0.371	0.405	1.60	−1.72	1.4693	0.84
MHPOCBC	0.001	378.070	4.332	0.922	−0.301	1.059	[0]	[0]	0.6298	1.00
	0.003	[378.070]	4.568	0.931	−0.220	0.750	[0]	[0]	0.6642	2.01
	0.01	[378.070]	5.408	0.949	−0.181	0.354	[0]	[0]	0.7855	5.35
	0.003	[378.070]	4.448	0.921	−0.492	1.410	4.16	−8.37	0.6456	1.19
	0.01	[378.070]	4.720	0.930	−0.332	0.990	1.53	−4.36	0.6852	2.18

diction $D_1^+\simeq D_1^-$ [37,38] with only exceptions of the cases $\lvert t\rvert_{\max}=0.01$ for MHPOBC and 12BIMF10. This violation might also be an indication of the crossover.

Fits were also tried holding the exponents fixed at the 3D XY values: $\alpha=-0.0066$ and $\theta=0.524$ [33]. Fits were made for both cases of fixing $D_2^\pm$ to zero and allowing $D_2^\pm$ to have nonzero values. At first, T_c was adjusted freely. However, it was found that the T_c values were rather unstable against data-range shrinking. For example, in MHPOBC when $D_2^\pm=0$, $T_c=396.062$, 396.049, and 396.041 K for $\lvert t\rvert_{\max}=0.001$, 0.003, and 0.01, respectively. Using different T_c's for different data ranges is clearly inconsistent, and is likely to give artificially *good* fits. To avoid this, we fixed T_c to the value determined in the narrowest data range. The parameter values are shown in Table III. Since higher-order correction terms are expected to have a significant influence only away from T_c, fits with nonzero $D_2^\pm$ are presented for data with $\lvert t\rvert_{\max}=0.003$ and 0.01 but not for data with $\lvert t\rvert_{\max}=0.001$. When the second-order correction terms are neglected ($D_2^\pm=0$), the fits over the data range $\lvert t\rvert_{\max}=0.001$ are moderately good in the χ_ν^2 sense, while the fits become much worse for larger $\lvert t\rvert_{\max}$. Inclusion of the second-order correction term improves χ_ν^2 to acceptable values. The critical amplitude ratio A^-/A^+ agrees with the theoretical value for the 3D XY model, $A^-/A^+=0.971\pm0.013$ [33]. However, the violation of the scaling prediction $D_1^+\simeq D_1^-$ is still seen in all the cases. This tendency is irrespective of fixing $D_2^\pm$ to zero or allowing $D_2^\pm$ to have nonzero values. Imposing $D_1^+=D_1^-$ resulted in poor fits, for example, $\chi_\nu^2=64$ for $\lvert t\rvert_{\max}=0.001$ with $D_2^\pm=0$ in MHPOBC. Such a situation indicates that the inclusion of corrections-to-scaling terms does not explain the observed critical behavior in a consistent manner, which is another support of the occurrence of the crossover.

Next we analyzed the ΔC_p data with crossover scaling theory. We have followed the calculation presented by Rudnick and Nelson [14], and the derivation of the crossover expression is described in the Appendix. The expression used here for fitting the observed ΔC_p data is

$$\Delta C_p=\frac{A^+}{\alpha}\left[(1+a^+\lvert t\rvert^{-1/2})^{2\alpha}-1\right]+B_c \tag{3}$$

for $t>0$, and

$$\Delta C_p=\frac{A^+}{\alpha}\left[(1+a^+\lvert 2t\rvert^{-1/2})^{2\alpha}-1\right]+10A^+(1+a^+\lvert 2t\rvert^{-1/2})^{2\alpha}\times\left[1+\frac{3\lvert t\rvert}{2a_u^2}(1+a^+\lvert 2t\rvert^{-1/2})^{y}\right]^{-1/2}+B_c \tag{4}$$

for $t<0$. The critical constant term B_c has been included. The exponent α is fixed to the 3D XY value -0.0066. As mentioned in the Appendix, the exponent y is here an adjustable parameter. We fixed y to -0.5 in all the fits shown below, because χ_ν^2 showed a broad minimum around this value.

The parameter values are summarized in Table IV. The fits are moderately good for $\lvert t\rvert_{\max}\leqslant 0.003$ in MHPOBC and 12BIMF10, and for $\lvert t\rvert_{\max}\leqslant 0.01$ in MHPBC and MHPOCBC. In Figs. 1–4, solid lines show the fit for $\lvert t\rvert_{\max}=0.01$. A comparison of the crossover fits shown here and the 3D XY fits with $D_2^\pm=0$ deserves attention, since they contain the same number of adjustable parameters. We see

TABLE IV. Least-squares values of the adjustable parameters for fitting ΔC_p with Eqs. (3) and (4). Quantities in brackets were held fixed at the given values. The units for A^+ and B_c are J K^{-1} g^{-1}.

System	$\lvert t\rvert_{\max}$	T_c	10^3A^+	a^+	a_u	B_c	E^+	E^-	χ^2_ν
MHPOBC	0.001	396.072	21.470	0.0233	0.0207	0.0086	[0]	[0]	2.56
	0.003	[396.072]	20.709	0.0287	0.0225	0.0044	[0]	[0]	2.93
	0.01	[396.072]	19.556	0.0529	0.0242	−0.0079	[0]	[0]	4.74
12BIMF10	0.001	329.072	42.027	0.0170	0.0191	0.0059	[0]	[0]	1.06
	0.003	[329.072]	41.363	0.0246	0.0192	−0.0082	[0]	[0]	3.20
	0.01	[329.072]	39.463	0.0419	0.0194	−0.0251	[0]	[0]	10.33
MHPBC	0.001	350.065	6.709	0.093	0.0238	−0.0081	[0]	[0]	2.34
	0.003	[350.065]	6.541	0.056	0.0285	−0.0025	[0]	[0]	2.16
	0.01	[350.065]	6.411	0.083	0.0289	−0.0059	[0]	[0]	1.68
MHPOCBC	0.001	378.071	4.697	0.0214	0.0271	0.0028	[0]	[0]	1.00
	0.003	[378.071]	4.627	0.0299	0.0285	0.0011	[0]	[0]	1.33
	0.01	[378.071]	4.491	0.0532	0.0293	−0.0018	[0]	[0]	2.69
MHPOBC	0.01	[396.072]	20.733	0.0247	0.0225	0.0088	−1.315	−0.949	2.28
12BIMF10	0.01	[329.072]	40.903	0.0212	0.0201	−0.0008	−1.211	−4.239	1.09
MHPBC	0.01	[350.065]	6.497	0.052	0.0292	−0.0016	−0.258	−0.290	1.61
MHPOCBC	0.01	[378.071]	4.581	0.0239	0.0298	0.0024	−0.285	−0.458	2.01

that the crossover fits are clearly better for MHPOBC, 12BIMF10, and MHPOCBC. In the case of MHPBC, the fits are equally good. We also tried fits adding a term $E^{\pm}|t|$ to Eqs. (3) and (4). The results are shown in the last four lines in Table IV. These results can be compared with the *XY* fits with nonzero $D_2^{\pm}$, which again contain an equal number of adjustable parameters. The crossover fits are clearly better in the χ^2_ν sense for MHPOBC and 12BIMF10, while the fits are equally good for MHPBC and MHPOCBC.

IV. DISCUSSION

To summarize the above results, we have seen that the ΔC_p data for the four systems studied here can be described by the scaling crossover expression. On the other hand, fits with the 3D *XY* model with correction-to-scaling terms but without crossover effect seem unsuccessful not only because they are worse than the crossover fits in the χ^2_ν sense in most cases, but also because of the violation of the theoretical prediction $D_1^+ \simeq D_1^-$.

In the crossover theory used here, there are two parameters a^+ and a_u which describe the crossover behavior. The temperature where the crossover from 3D *XY* to the tricritical behavior is given by $t_{co}=(a^+)^2$. If we exclude relatively poor fits such as $|t|_{\max}=0.01$ with $E^{\pm}=0$ in MHPOBC, we see from Table IV that a^+ values are more or less alike for MHPOBC, 12BIMF10, and MHPOCBC: $a^+ \simeq 0.02-0.03$, while it is slightly larger in MHPBC: $a^+ \simeq 0.05-0.09$. This indicates that the crossover to tricritical behavior is least remarkable in MHPBC, which is consistent with the observation that the increase in α with $|t|_{\max}$ obtained in the α-free fits is least significant in MHPBC as shown in Table II.

The parameter a_u measures the crossover from ordinary second-order to the tricritical behavior of the underlying Landau anomaly. In the absence of fluctuation effects, ΔC_p would exhibit a typical mean-field cusp anomaly with a full width at half height $t_0=2a_u^2$. The values of a_u listed in Table IV yield $t_0 \simeq (0.7-2.2)\times 10^{-3}$. These are comparable with the values reported for the liquid-crystal systems showing Landau-like Sm-A–Sm-C (or C^*) transitions [39,40]. This indicates that a large sixth-order term is quite a common feature among Sm-A–Sm-C (or C^*) transitions.

In the tricritical regime where $|t| \gg (a^+)^2$ and $|t| \gg a_u^2$, Eqs. (3) and (4) become

$$\Delta C_p \simeq 2a^+A^+|t|^{-1/2}+B_c, \tag{5}$$

$$\Delta C_p \simeq \left[2a^+A^+2^{-1/2}+10A^+a_u\left(\frac{3}{2}\right)^{-1/2}\right]|t|^{-1/2}+B_c. \tag{6}$$

Hence the amplitude ratio in the tricritical regime is given by

$$r_t = 2^{-1/2}+5\left(\frac{3}{2}\right)^{-1/2}\frac{a_u}{a^+} \tag{7}$$

$$= 2^{-1/2}+5\left(\frac{3}{2}\right)^{-1/2}v^{-1/2}. \tag{8}$$

We see that this ratio is system dependent, in agreement with the theoretical expectation [13,41]. As the system approaches the classical limit, the coefficient of the gradient term in the bare Hamiltonian becomes larger, so that v in the scaled Hamiltonian [see Eq. (A1)] approaches zero and therefore r_t diverges, as expected. From the values listed in Table IV we obtain $r_t \simeq 4-6$ for MHPOBC, 12BIMF, and MHPOCBC. These values are close to the value $r_t \simeq 7-9$ found for the racemate MHPOBC [12], but clearly larger than $r_t \simeq 1.0-1.6$ reported for N–Sm-A tricritical systems [20–22]. On the other hand, we obtain $r_t \simeq 2-3$ for MHPBC, which lies in between.

In our previous work [30], we reported the results of preliminary analysis of the ΔC_p data. The crossover expression for $T>T_c$ [Eq. (7) of Ref. [30]] was essentially the same as

the one used in the present analysis, although it was derived in a different way there. For $T<T_c$, we assumed that the heat-capacity anomaly can be written as a simple sum of the critical part and the Landau part [Eq. (10) of Ref. [30]]. Because this assumption had no theoretical basis, the high quality of the fits found there ($\chi_\nu^2 \simeq 1.6-1.8$ for $|t|_{\max}=0.01$) should be viewed as having an empirical significance rather than a theoretical one.

Since examples of clear crossover between tricritical and critical behavior are quite limited, it is of special interest to study physical quantities other than the heat capacity for this family of antiferroelectric liquid crystals. In particular, the measurement of the correlation length is of great value. One advantage is that the correlation length has the exponent values substantially different from each other for the XY ($\nu_{XY}=0.6689$) and the tricritical cases ($\nu_t=0.5$), and they are distinguished easily. Furthermore, a relatively short bare correlation length expected from the significant fluctuation effect in the ΔC_p data can be verified by such measurement.

ACKNOWLEDGMENTS

We wish to express our sincere thanks to Professor H. Takezoe for supplying us high-quality liquid-crystal samples, and to Professor C. W. Garland for helpful discussions and critical reading of the manuscript. We are also grateful to Professor A. Aharony, Professor M. E. Fisher, Professor T. Lubensky, and Professor D. Nelson for valuable discussions.

APPENDIX: DERIVATION OF CROSSOVER SCALING EXPRESSION

For analyzing the present data, we need a crossover scaling function of the heat capacity both above and below T_c. We also have to include the sixth-order term which is necessary to describe the heat-capacity anomaly at the Sm-A–Sm-C transition. Although there has been no explicit calculation which satisfies these requirements, we can follow Rudnick and Nelson [14], who have established the basic procedure of such an approach. They started from the Landau-Ginzburg-Wilson Hamiltonian for isotropic n-component spins in d dimensions:

$$\mathcal{H}=\int dR[\tfrac{1}{2}(\nabla\vec{S})^2+\tfrac{1}{2}r|\vec{S}|^2+u|\vec{S}|^4+v|\vec{S}|^6]. \quad \text{(A1)}$$

Hereafter, we confine ourselves to the case $d=3$ so that $\epsilon=4-d=1$.

Rudnick and Nelson carried out calculation to the leading order neglecting the sixth-order term in Eq. (A1). Above T_c, this result is still adequate for our purpose. The singular part of the heat capacity, $\Delta C_p^{\rm sing}$, is given as

$$\Delta C_p^{\rm sing}=\frac{nK_4}{2B(1-2A/B)u}[Q^{1-2A/B}-1], \quad \text{(A2)}$$

where

$$Q=1+Bu|\tau|^{-1/2}, \quad \text{(A3)}$$

with

$$A=4(n+2)K_4, \quad B=4(n+8)K_4, \quad K_4=1/(8\pi^2). \quad \text{(A4)}$$

We use τ as the ''temperature'' because it is not necessarily equal to the experimentally obtained reduced temperature t while it is proportional to t.

Near T_c, where $|\tau|\ll(Bu)^2$, Q behaves like $|\tau|^{-1/2}$, so that

$$\Delta C_p^{\rm sing}\sim|\tau|^{-0.5+A/B}. \quad \text{(A5)}$$

Hence the critical exponent is

$$\alpha=0.5-\frac{A}{B}=\frac{1}{2}\left(\frac{4-n}{n+8}\right), \quad \text{(A6)}$$

yielding a positive value for $n=2$, as in the ϵ expansion to first order, which disagrees with the result obtained by more precise theoretical calculations. Our remedy here is to put the overall error into the value A, and replace the factor $(1-2A/B)$ by the more accurate exponent value $2\alpha_{XY}=-0.0132$. We obtain instead of Eq. (A2)

$$\Delta C_p^{\rm sing}=\frac{nK_4}{4\alpha Bu}[Q^{2\alpha}-1]. \quad \text{(A7)}$$

Below T_c, we proceed in a way similar to that used by Rudnick and Nelson, except that here we retain the sixth-order term. The singular heat capacity can be written as

$$\Delta C_p^{\rm sing}=\Delta C_p^{(1)}+\Delta C_p^{(2)}. \quad \text{(A8)}$$

Here $\Delta C_p^{(1)}$ is given by the same expression with that for $T>T_c$, Eqs. (A2) and (A3), except that $|\tau|$ should be replaced by $-2\tau=|2\tau|$ [42]. On the other hand, $\Delta C_p^{(2)}$ comes from the part of the free energy which is dependent on the order parameter M:

$$F(M)=\frac{1}{2}\tau_R M^2+u_R M^4+v_R M^6, \quad \text{(A9)}$$

where

$$\tau_R=\tau Q^{-A/B}, \quad u_R=uQ^{-1}, \quad v_R=vQ^{x_v}. \quad \text{(A10)}$$

The power x_v has a value -5 for $n=1$ to order ϵ [13,43]. Instead of using the value for $n=2$ which is available in the same accuracy, we treat x_v as an adjustable parameter because it might contain some error of the same type as mentioned above for the value of A/B. After minimization with respect to M, the heat capacity is obtained by differentiating twice with τ. Neglecting the relatively weak τ-dependence through Q, we obtain [44]

$$\Delta C_p^{(2)}=\frac{1}{8u}Q^{2\alpha}\left[1-\frac{3v\tau}{2u^2}Q^{1.5+\alpha-x_v}\right]^{-1/2}. \quad \text{(A11)}$$

We have replaced $1-2A/B$ by 2α as was done in obtaining Eq. (A7).

In summary, the experimentally observed singular heat capacity above and below T_c can be represented by

$$\Delta C_p^{\rm sing}=\frac{A^+}{\alpha}\left[(1+a^+|t|^{-1/2})^{2\alpha}-1\right] \tag{A12}$$

for $t>0$, and

$$\Delta C_p^{\rm sing}=\frac{A^+}{\alpha}[(1+a^+|2t|^{-1/2})^{2\alpha}-1] +A^M(1+a^+|2t|^{-1/2})^{2\alpha} \times\left[1+\frac{3|t|}{2a_u^2}(1+a^+|2t|^{-1/2})^{y}\right]^{-1/2} \tag{A13}$$

for $t<0$. Here,

$$y=1.5+\alpha-x_v\,, \tag{A14}$$

$$\tau=\theta t, \tag{A15}$$

$$a^+=Bu\,\theta^{-1/2}, \tag{A16}$$

$$a_u=uv^{-1/2}\theta^{-1/2}, \tag{A17}$$

$$A^+=\frac{nK_4A_0}{4Bu}, \tag{A18}$$

$$A^M=\frac{A_0}{8u}, \tag{A19}$$

where A_0 is the proportionality constant between the theoretically calculated and the experimentally observed heat capacity. With Eq. (A4) and $n=2$ we further obtain from Eqs. (A18) and (A19) $A^+=A_0/80u$ so that

$$A^M=10A^+. \tag{A20}$$

It is easily seen that the $\Delta C_p^{\rm sing}$ for both above and below T_c reduces to the purely tricritical behavior in the limit $u\to 0$ so that a_u also goes to zero, as expected. On the other hand, putting $v\to 0$ with finite u reduces Eq. (A13) to the same form as obtained by Rudnick and Nelson.

[1] P. G. de Gennes, Mol. Cryst. Liq. Cryst. **21**, 49 (1973).
[2] C. C. Huang and J. M. Viner, Phys. Rev. A **25**, 3385 (1982).
[3] C. C. Huang and S. Dumrongrattana, Phys. Rev. A **34**, 5020 (1986).
[4] T. Chan, Ch. Bahr, G. Heppke, and C. W. Garland, Liq. Cryst. **13**, 667 (1993).
[5] F. Yang, G. W. Bradberry, and J. R. Sambles, Phys. Rev. E **50**, 2834 (1994).
[6] C. R. Safinya, M. Kaplan, J. Als-Nielsen, R. J. Birgeneau, D. Davidov, J. D. Litster, D. L. Johnson, and M. E. Neubert, Phys. Rev. B **21**, 4149 (1980).
[7] V. L. Ginsburg, Fiz. Tverd. Tela (Leningrad) **2**, 2031 (1960) [Sov. Phys. Solid State **2**, 1824 (1960)].
[8] K. Ema, J. Watanabe, A. Takagi, and H. Yao, Phys. Rev. E **52**, 1216 (1995).
[9] K. Ema, H. Yao, A. Fukuda, Y. Takanishi, and H. Takezoe, Phys. Rev. E **54**, 4450 (1996).
[10] K. Ema, H. Yao, and K. Itoh, Ferroelectrics **178**, 221 (1996).
[11] L. Reed, T. Stoebe, and C. C. Huang, Phys. Rev. E **52**, R2157 (1995).
[12] It was found that racemate of MHPOBC exhibits a non-Landau tricritical Sm-*A*–Sm-*C* transition. See K. Ema, A. Takagi, and H. Yao, Phys. Rev. E **53**, R3036 (1996); **55**, 508 (1997).
[13] I. D. Lawrie and S. Sarbach, in *Phase Transitions and Critical Phenomena*, edited by C. Domb and J. L. Lebowitz (Academic, New York, 1984), Vol. 9.
[14] D. R. Nelson and J. Rudnick, Phys. Rev. Lett. **35**, 178 (1975); J. Rudnick and D. R. Nelson, Phys. Rev. B **13**, 2208 (1976).
[15] M. B. Salamon and H.-T. Shang, Phys. Rev. Lett. **44**, 879 (1980); H.-T. Shang and M. B. Salamon, Phys. Rev. B **22**, 4401 (1980).
[16] N. Giordano and W. P. Wolf, Phys. Rev. Lett. **39**, 342 (1977).
[17] E. K. Riedel, H. Meyer, and R. P. Behringer, J. Low Temp. Phys. **22**, 369 (1976).
[18] T. Takada and T. Watanabe, J. Low Temp. Phys. **41**, 221 (1980).
[19] B. M. Ocko, R. J. Birgeneau, and J. D. Litster, Z. Phys. B **62**, 487 (1986), and references cited therin.
[20] J. Thoen, H. Marynissen, and W. Van Dael, Phys. Rev. Lett. **52**, 204 (1984), and references therein.
[21] K. Stine and C. W. Garland, Phys. Rev. A **39**, 3148 (1989).
[22] G. Nounesis, C. W. Garland, and R. Shashidhar, Phys. Rev. A **43**, 1849 (1991).
[23] C. W. Garland and G. Nounesis, Phys. Rev. E **49**, 2964 (1994).
[24] M. E. Fisher, Phys. Rev. **176**, 257 (1968).
[25] We note that the racemic mixture is an exceptional case. This is because Fisher renormalization depends on $d(\ln T_c)/dX$ being large, and $d(\ln T_c)/dX=0$ for racemates.
[26] A. D. L. Chandani, Y. Ouchi, H. Takezoe, A. Fukuda, K. Terashima, K. Furukawa, and A. Kishi, Jpn. J. Appl. Phys., Part 2 **28**, L1261 (1989); Y. Takanishi, K. Hiraoka, V. K. Agrawal, H. Takezoe, A. Fukuda, and M. Matsushita, Jpn. J. Appl. Phys. Part 1 **30**, 2023 (1991); K. Hiraoka, Y. Takanishi, K. Skarp, H. Takezoe, and A. Fukuda, Jpn. J. Appl. J. Phys. Part 2 **30**, L1819 (1991).
[27] N. Okabe, Y. Suzuki, I. Kawamura, T. Isozaki, H. Takezoe, and A. Fukuda, Jpn. J. Appl. Phys., Part 2 **31**, L793 (1992).
[28] T. Isozaki, Y. Suzuki, I. Kawamura, K. Mori, N. Yamamoto, Y. Yamada, H. Orihara, and Y. Ishibashi, Jpn. J. Appl. Phys., Part 2 **30**, L1573 (1991); T. Isozaki, K. Hiraoka, Y. Takanishi, H. Takezoe, A. Fukuda, Y. Suzuki, and I. Kawamura, Liq. Cryst. **12**, 59 (1992).
[29] K. Itoh, M. Kabe, K. Miyachi, Y. Takanishi, K. Ishikawa, H. Takezoe, and A. Fukuda, J. Mater. Chem. **7**, 407 (1997).
[30] K. Ema, M. Ogawa, A. Takagi, and H. Yao, Phys. Rev. E **54**, R25 (1996).
[31] K. Ema, T. Uematsu, A. Sugata, and H. Yao, Jpn. J. Appl. Phys., Part 1 **32**, 1846 (1993).
[32] Because of an insufficient calibration of the thermometer used just after the completion of the improved calorimeter, it was found that the temperature scale should be shifted by about 0.4 K in the results of Ref. [8].
[33] C. Bagnuls and C. Bervillier, Phys. Rev. B **32**, 7209 (1985); C.

ÅBervillier, *ibid.* **34**, 8141 (1986); C. Bagnuls, C. Bervillier, D. I. Meiron, and B. G. Nickel, Phys. Rev. B **35**, 3585 (1987).
[34] The theory in Ref. [33] has been applied for the $N-$Sm-A transition in C. W. Garland, G. Nounesis, M. J. Young, and R. J. Birgeneau, Phys. Rev. E **47**, 1918 (1993).
[35] S. Y. Zinn and M. F. Fisher, Physica A **226**, 168 (1996).
[36] H. Haga, A. Onodera, Y. Shiozaki, K. Ema, and H. Sakata, J. Phys. Soc. Jpn. **64**, 822 (1995).
[37] $D_1^+ = D_1^-$ is expected in the ϵ-expansion calculation to leading order ϵ. See A. Aharony and G. Ahlers, Phys. Rev. Lett. **44**, 782 (1980).
[38] The values of D_1^+/D_1^- obtained in the ϵ expansion up to higher order and in the field theory are only slightly larger than unity for 3D XY universality class: 1.17 and 1.6, respectively. See V. Privman, P. C. Hohenberg, and A. Aharony, in *Phase Transitions and Critical Phenomena*, edited by C. Domb and J. L. Lebowitz (Academic, New York, 1991), Vol. 14.
[39] M. Michle and C. W. Garland, Phys. Rev. A **27**, 2624 (1983).
[40] S. C. Lien and C. C. Huang, Phys. Rev. A **30**, 624 (1984); C. C. Huang and S. C. Lien, *ibid.* **31**, 2621 (1985).
[41] M. E. Fisher and S. Sarbach, Phys. Rev. Lett. **41**, 1127 (1978); S. Sarbach and M. E. Fisher, Phys. Rev. B **20**, 2797 (1979).
[42] To be precise, τ should be replaced by $\sigma\tau$ rather than -2τ, where σ is determined in a consistent manner at each temperature. If $v=0$ then $\sigma=-2$ for all τ. For nonzero v, σ takes a value between -3 and -2. However, we found that the dependence of σ on τ yields only small effect and can be neglected practically in fitting the experimental data.
[43] Also see, for instance, I. D. Lawrie, J. Phys. A **12**, 919 (1979).
[44] We also tried fits by numerically differentiating $F(M)$ by τ. The result was essentially the same.